BIOCHEMISTRY
including biophysical chemistry & molecular biology

Article

pubs.acs.org/biochemistry

The Lys-Specific Molecular Tweezer, CLR01, Modulates Aggregation of the Mutant p53 DNA Binding Domain and Inhibits Its Toxicity

Gal Herzog,[†] Merav D. Shmueli,[†] Limor Levy,[†] Liat Engel,[†] Ehud Gazit,[†] Frank-Gerrit Klärner,[‡] Thomas Schrader,[‡] Gal Bitan,[§] and Daniel Segal*[,†]

[†]Department of Molecular Microbiology and Biotechnology, George S. Wise Faculty of Life Sciences, Tel Aviv University, Ramat Aviv, Israel 69978

[‡]Institute of Organic Chemistry, University of Duisburg-Essen, 45117 Essen, Germany

[§]Department of Neurology, David Geffen School of Medicine, Brain Research Institute, and Molecular Biology Institute, University of California at Los Angeles, Los Angeles, California 90095-7334, United States

Supporting Information

ABSTRACT: The tumor suppressor p53 plays a unique role as a central hub of numerous cell proliferation and apoptotic pathways, and its malfunction due to mutations is a major cause of various malignancies. Therefore, it serves as an attractive target for developing novel anticancer therapeutics. Because of its intrinsically unstable DNA binding domain, p53 unfolds rapidly at physiological temperature. Certain mutants shift the equilibrium toward the unfolded state and yield high-molecular weight, nonfunctional, and cytotoxic β-sheet-rich aggregates that share tinctorial and conformational similarities with amyloid deposits found in various protein misfolding diseases. Here, we examined the effect of a novel protein assembly modulator, the lysine (Lys)-specific molecular tweezer, CLR01, on different aggregation stages of misfolded mutant p53 *in vitro* and on the cytotoxicity of the resulting p53 aggregates in cell culture. We found that CLR01 induced rapid formation of β-sheet-rich, intermediate-size p53 aggregates yet inhibited further p53 aggregation and reduced the cytotoxicity of the resulting aggregates. Our data suggest that aggregation modulators, such as CLR01, could prevent the formation of toxic p53 aggregates.

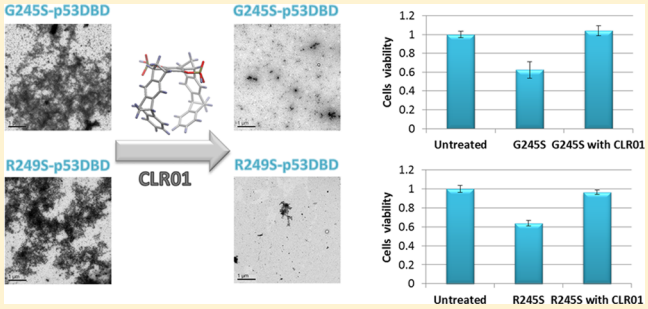

p53 is a transcription factor that regulates the cell cycle and plays a key role in the prevention of cancer development.[1] The outstanding role of p53 as a tumor suppressor and its unique location as a hub of numerous cell pathways make it a prime target for developing novel anticancer therapeutics.

p53 functions as a homotetramer, comprising four polypeptide chains of 393 amino acid residues each. The structure of p53 consists of two folded domains, the DNA binding domain (DBD) and the oligomerization domain (OD), which are flanked by intrinsically disordered domains, the transactivation domain (TAD) in the N-terminus and a regulatory domain at the extreme C-terminus (CTD). The p53DBD is intrinsically unstable and unfolds rapidly at body temperature.[2,3]

Folded and unfolded p53 are in equilibrium, but unfolded p53 can denature irreversibly and form small, soluble aggregates, which subsequently assemble irreversibly by classical nucleation-dependent polymerization, displaying typical kinetics characterized by a lag phase, followed by a rapid growth and finally a plateau (Figure 1).[3−5] This process is facilitated by multiple distinct mutations and eventually yields high-molecular weight, β-sheet-rich aggregates that are conformationally and tinctorially similar to the amyloid deposits characterizing many protein misfolding diseases, although their morphology tends to be amorphous rather than fibrillar.[5−7]

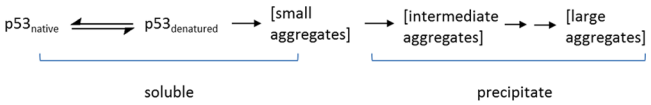

Figure 1. Illustration of the process of denaturation and subsequent aggregation of p53. Folded and unfolded p53 are in equilibrium, but unfolded p53 can irreversibly denature and form small, soluble aggregates, which cluster and precipitate over time. Adapted from ref 3.

Because the DBD governs the stability of the entire protein and is responsible for its transcriptional transactivation, >90% of the oncogenic mutations in p53 have been found to be located in this domain.[8] Of all p53-associated cancer mutations, 30−40% perturb the structure of the protein (conformational mutations), resulting in reduced thermostability and leading to an increased aggregation rate.[3,9] Two such examples are the mutations leading to G245S and R249S substitutions in the

Received: August 29, 2014
Revised: May 20, 2015
Published: June 1, 2015

DOI: 10.1021/bi501092p
Biochemistry 2015, 54, 3729−3738

p53DBD, which are two of the six most frequent conformational mutations in human cancers.[9] These two mutants and other conformational mutants of p53 largely are unfolded under physiological conditions, thus displaying a loss of transcription transactivation capacity.[10] The G245S and R249S substitutions induce conformational changes in the DBD and destabilize the protein moderately by only 1−2 kcal/mol.[8]

The G245S and R249S structural variants of p53 result from two of the most frequent mutations in the p53 cognate gene found in cancer patients. These mutations are located in the L3 loop, which binds to the minor groove of DNA response elements.[11] The crystal structure of G245S-p53DBD revealed distinct structural changes in the immediate environment of the mutation site. Observed conformational changes in certain surface loops (e.g., the L1 and S7−S8 loops) can be attributed to differences in crystallization conditions and crystal packing for wild-type (WT) p53DBD and G245S-p53DBD. In contrast, the R249S mutation substantially perturbs the L3 loop, induces high flexibility, and favors alternative conformations with substantially more severe consequences for overall protein stability and DNA binding.[11] These structural changes in the p53DBD also result in the high propensity of G245S and R249S to aggregate.[3]

Although a large body of structural information is available on the transition of p53 mutants from the folded to the unfolded state, much less is known about the shift from the unfolded to the "small aggregate" state. It is thus reasonable to believe that because G245S-p53DBD and R249S-p53DBD adopt alternative conformations in the unfolded state they also possess different structures at the initiation of aggregation.

In addition to being nonfunctional, structural p53 mutants also have been reported to impart a dominant-negative effect over the wild-type protein. A recent landmark paper has uncovered a novel mechanism for this dominant-negative effect. Rousseau, Schymkowitz, and co-workers found that the structural mutations expose an aggregation-nucleating sequence, which normally is buried in the hydrophobic core of the DBD of p53. As a result, these mutant proteins have an increased propensity to form amyloid-like aggregates.[12] In addition, these aggregates recruit wild-type p53 into cellular inclusions, thereby decreasing the normal p53 availability and accounting for the dominant-negative effect of the mutant. Moreover, structurally destabilized p53 mutants also co-aggregate with p53 family members p63 and p73, thereby accounting for their loss of function.[12]

Interestingly, it has been shown recently that preformed p53 aggregates enter HeLa cells via macropinocytosis, a nonspecific pathway, and induce intracellular aggregation of endogenous p53.[13] Although the clinical significance of this observation remains to be elucidated, these data suggest a possible role for p53 aggregation in cancer development that is distinct from direct loss of function of p53 by mutation. Thus, interfering with the aggregation of p53 mutants by small-molecule modulators may prevent the harmful effects of the resulting aggregates and co-aggregation with WT p53, p63, and p73. However, rescuing folding and function of p53 mutants by a specific ligand represents a great challenge because only a few of these mutants (e.g., Y220C) possess a cleft or a crevice that can be targeted by a small molecule without interfering with the ability of p53 to bind its DNA response element.[11] An alternative strategy is to modulate the aggregation itself. Theoretically, if a small molecule could prevent the formation of the amyloid-like aggregates, it might both prevent the potential toxicity of these aggregates and inhibit the recruitment of WT p53, p63, and p73 into the aggregates.

Recently, a novel family of protein assembly modulators, namely lysine (Lys)-specific molecular tweezers (MTs), was found to consist of highly efficient inhibitors of amyloid assembly and toxicity.[14] These small molecules are horseshoe-shaped, artificial Lys receptors composed of two hydrocarbon arms capable of hydrophobic interactions with the alkyl side chains of Lys residues, and negatively charged headgroups that form electrostatic interactions with the NH_3^+ group of Lys (Figure 2).

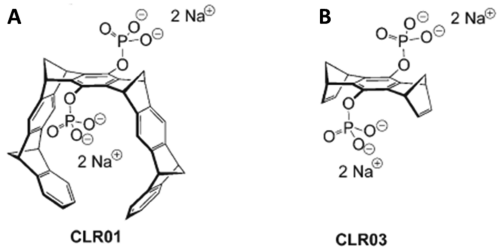

Figure 2. Structures of molecular tweezers (A) CLR01 and (B) CLR03. Reprinted with permission from ref 14. Copyright 2011 American Chemical Society.

Inhibition of aggregation by MTs is selective for amyloidogenic proteins but is not specific to a particular protein.[15] For example, the MT, CLR01 (Figure 2A), disrupted *in vitro* the aggregation and toxicity of multiple disease-related proteins, such as amyloid β-protein (Aβ), tau, and α-synuclein at equimolar or subequimolar concentration ratios,[14] whereas disruption of tubulin polymerization required an ∼55-fold excess of CLR01,[15] and inhibition of enzymatic activity, e.g., of alcohol dehydrogenase, required an ∼850-fold excess of CLR01.[16] In agreement with these observations, *in vivo* CLR01 suppressed α-synuclein aggregation in neurons and rescued the phenotype and survival of zebrafish embryos, cleared existing Aβ and tau aggregates in the brain of Alzheimer's disease transgenic mice, and decreased the level of transthyretin aggregation in a mouse model of familial amyloidotic polyneuropathy, without any side effects.[17−19] Moreover, CLR01 was found to have a high safety margin in mice,[15] supporting its selective action as an inhibitor of abnormal protein aggregation.

Here, we examined the effect of CLR01 on different stages of aggregation of the p53 mutants G245S and R249S *in vitro* and on the harmful effect of their preformed aggregates in cultured lung carcinoma cells. We found that CLR01 induced rapid formation of β-sheet-rich, intermediate-size aggregates by each p53DBD mutant, inhibited formation of later aggregates, and reduced the cytotoxicity of the resulting aggregates.

MATERIALS AND METHODS

The Na^+ salts of CLR01 and CLR03 were prepared and purified like the Li salts, as described previously.[16]

Cloning. The coding sequence of the gene encoding the human p53DBD was amplified using the primers 5′-GGGAATTCGGATCCATGTCATCTTCTGTCCCTTCCCAG-3′ and 5′-TCTGACCTCGAGTCAGGTGTTGTTGGACAGTGCTCGC-3′. The G245S-p53DBD or R249S-p53DBD mutant was generated by polymerase chain reaction (PCR) site-

DOI: 10.1021/bi501092p
Biochemistry 2015, 54, 3729−3738

directed mutagenesis using the primer 5′-CTGCATGGGCaG-CATGAACC-3′ or 5′-CATGAACCGGAGcCCCATC-3′, respectively (a lowercase letter indicates the substitution made to produce the mutation). The PCR products were digested with *Bam*HI and *Xho*I, purified, and cloned into a modified pET24a+ expression vector. The resulting plasmids encoded fusion proteins comprising an N-terminal six-His tag, the lipoyl domain of the dihydrolipoamide acetyltransferase from *Bacillus stearothermophilus*, and a TEV protease cleavage site followed by the p53DBD.

Protein Expression and Purification. The appropriate vector was transformed into competent *Escherichia coli* BL21 tuner cells (Novagen) for overexpression. Expression cultures were incubated at 37 °C while being shaken at 220 rpm until OD_{600} reached 0.7−0.8. The medium was supplemented with 0.1 mM $ZnSO_4$, and expression was induced with 0.5 mM isopropyl β-D-1-thiogalactopyranoside at 18 °C. Cells were harvested 14 h later by centrifugation. The cell pellet from 3 L of culture was suspended in 50 mM Tris-HCl (pH 7.2), 200 mM NaCl, 0.8% Triton, 10% glycerol, 5 mM imidazole, 10 mM β-mercaptoethanol, and X50 tablets of EDTA-free complete protease inhibitor (Roche). Cells were sonicated on ice for a total time of 8 min, with 90 s in between 30 s pulses. The soluble fraction was loaded onto an Amersham 26/20 column packed with Ni-Sepharose (GE Healthcare). The His-tagged fusion protein was eluted using a 0 to 500 mM imidazole gradient over 10 column volumes. The pooled fractions from the Ni-Sepharose column were digested with TEV protease overnight and dialyzed against a low-salt buffer containing 50 mM Tris-HCl (pH 7.2), 50 mM NaCl, 10% glycerol, and 10 mM β-mercaptoethanol. The dialyzed sample was purified further on a HiPrep Heparin 16/10 FF ion-exchange column (GE Healthcare). Elution was conducted using a 0 to 500 mM NaCl gradient over 10 column volumes. The pooled fractions were concentrated using an Amicon ultra-15 instrument with a 30 kDa cutoff (Millipore) and buffer-exchanged to 25 mM sodium phosphate (pH 7.2), 10% glycerol, 300 mM NaCl, and 1 mM tris(2-carboxyethyl)phosphine (TCEP). To obtain high-purity proteins, a final gel-filtration step was conducted. The gel-filtration column (Superdex 75 HiLoad 16/60, GE Healthcare) was equilibrated with 25 mM sodium phosphate (pH 7.2), 10% glycerol, 300 mM NaCl, and 1 mM TCEP. The loading volume of concentrated proteins was 0.5 mL per run. Separation was performed by running 1.5 column volumes of the buffer and collecting 0.5 mL fractions. Protein samples were flash-frozen and stored in liquid nitrogen for further use. The purified p53 variants were verified by Western blot analysis under denaturing conditions using an anti-p53 monoclonal antibody (PAb 240, Abcam).

Differential Scanning Fluorimetry (DSF). Experiments were performed using SYPRO Orange (Invitrogen) as the fluorescent probe, which binds quantitatively to the hydrophobic protein patches exposed upon thermal denaturation. Real-time melting analysis was performed using a Corbett Rotor-Gene 6000 real-time qPCR thermocycler. The excitation (λ_{ex}) and emission (λ_{em}) wavelengths used were 460 and 510 nm, respectively. Heating from 28 to 70 °C was applied at a constant heating rate of 250 °C/h. Protein (10 μM) was briefly mixed with SYPRO orange (10×) in 25 mM sodium phosphate buffer (pH 7.2), 300 mM NaCl, 10% glycerol, 10% DMSO, and 1 mM TCEP. The apparent melting temperature (T_m) of the protein was determined from the inflection point of the melting curve.

Static Light Scattering (SLS). Protein aggregation was monitored by measuring static light scattering at 500 nm as excitation and emission wavelengths (excitation slit width of 0.8 nm, emission slit width of 2 nm) using a Horiba (Kyoto, Japan) FluoroMax-3 spectrophotometer. Experiments were performed using G245S-p53DBD or R249S-p53DBD at a concentration of 3 μM in 25 mM sodium phosphate (pH 7.2), 300 mM NaCl, 5% DMSO, and 1 mM TCEP buffer that was pre-equilibrated for 30 min at 37 °C. The samples were stirred constantly. Data were analyzed using Kaleidagraph (Synergy).

Thioflavin-T (ThT) Assay. ThT fluorescence was measured at 482 nm upon excitation at 450 nm for detecting β-sheet formation (excitation slit width of 3 nm, emission slit width of 4 nm), using a Horiba FluoroMax-3 spectrofluorometer. Time-resolved fluorescence was recorded immediately after adding 3 μM G245S-p53DBD or R249S-p53DBD protein to pre-equilibrated buffer [25 mM sodium phosphate (pH 7.2), 300 mM NaCl, 5% DMSO, 1 mM TCEP, and 10 μM ThT].

8-Anilino-1-naphthalene Sulfonic Acid (ANS) Binding Assay. ANS fluorescence was measured at 465 nm upon excitation at 350 nm for monitoring exposed hydrophobic regions in proteins, using a Horiba Jobin Yvon FL3-11 spectrofluorometer. Time-resolved fluorescence was recorded immediately after adding 5 μM G245S-p53DBD or R249S-p53DBD protein to pre-equilibrated buffer [25 mM sodium phosphate (pH 7.2), 300 mM NaCl, 5% DMSO, 1 mM TCEP, different concentrations of the tested compounds, and 5 μM ANS].

Circular Dichroism (CD) Measurements. CD spectra in the far-UV region (200−250 nm) were recorded with a Chirascan CD spectrometer (Applied Photophysics) equipped with a temperature-controlled cell using a cell with a path length of 0.5 cm. The bandwidth was 1 nm, and the averaging time was 30 s for each measurement. The protein concentration was 5 μM in a buffer containing 25 mM sodium phosphate (pH 7.2), 100 mM NaCl, 1 mM TCEP, and different concentrations of the tested compounds. The measurements were conducted at 37 °C after incubation for 20 min. The percentage of secondary structure was calculated using the CDNN software.[20]

Dot Blot. Spots (50 μL) containing 5 μM protein and different concentrations of the tested compounds, after incubation for 20 min at 37 °C, were applied, interspaced with spots containing only buffer, to a nitrocellulose membrane using a Minifold I Dot-Blot 96 Well Plate System (Whatman). The membrane was blocked for 1 h in the blocking solution [5% nonfat milk powder in Tris-buffered saline (TBS)] and then incubated in a 1:1000 dilution of the OC antibody (a generous gift from R. Kayed, University of Texas Medical Branch, Galveston, TX) in the blocking solution. The membrane was then washed three times for 15 min each in TTBS (0.1% Tween 20 in TBS), incubated for 40 min with the anti-rabbit secondary antibody, and washed three times for 10 min in TTBS. The membrane was developed using EZ-ECL (Biological Industries Ltd., Kibbutz Beit-Haemek, Israel), according to the manufacturer's instructions, and exposed to Fuji medical X-ray film for up to 5 min. Films were developed using Kodak X-OMAT 2000.

Turbidity Assay. The aggregation of G245S-p53DBD or R249S-p53DBD protein was monitored by absorbance reading at λ = 340 nm. Samples were incubated in 96-well plates in triplicate, each consisting of 5 μM protein dissolved in 25 mM sodium phosphate (pH 7.2), 300 mM NaCl, 5% DMSO, 1 mM TCEP, and different concentrations of the tested compound. A

DOI: 10.1021/bi501092p
Biochemistry 2015, 54, 3729−3738

similar set of samples, including only the tested compound, was measured in parallel for background turbidity subtraction. Plates were sealed and transferred immediately to an EL808 plate reader (BioTek). Aggregation was monitored for 2 h in 3 min intervals.

Transmission Electron Microscopy. G245S-p53DBD or R249S-p53DBD (5 μM) was incubated at 37 °C in 25 mM sodium phosphate (pH 7.2), 300 mM NaCl, 5% DMSO, 1 mM TCEP, and different concentrations of the tested compounds. Aliquots (5 μL) were taken after 45 min, adsorbed onto freshly glow-discharged carbon film, 400-mesh copper grids, rinsed with deionized water, and stained with 1% uranyl acetate. Images were taken using a Phillips 208S transmission electron microscope at 80 kV.

Cell Viability Assay. G245S-p53DBD or R249S-p53DBD aggregates (5 μM) were obtained by overnight incubation at 37 °C in the absence or presence of either CLR01 or CLR03 at different concentrations. The preformed aggregates were added to human H1299 non-small cell lung carcinoma cells and incubated for 24 h. Cell viability was measured using the 2,3-bis(2-methoxy-4-nitro-5-sulfophenyl)-2*H*-tetrazolium-5-carboxanilide (XTT) reduction assay according to the manufacturer's recommendations (Biological Industries Ltd.) with three wells per condition. As a negative control, CLR01 or CLR03 at different concentrations without G245S-p53DBD or R249S-p53DBD aggregates was added to cells. For a positive control, 0.1% Triton X-100 was used for induced cell lethality.

RESULTS

CLR01 Does Not Affect the Thermostability of the G245S-p53DBD Structural Mutant. Inactivation of p53 by denaturation involves the initial unfolding of the core domain, which occurs naturally but is reversible (Figure 1). It was shown previously that CLR01 had no stabilizing effect on other amyloidogenic proteins such as transthyretin (TTR).[19] Similarly, MTs would not be expected to stabilize the native conformation of p53; however, they could do that serendipitously, complicating data interpretation. Therefore, to rule out this possibility, CLR01 and the negative control derivative, CLR03 (Figure 2B), were tested *in vitro* for potential stabilizing effects toward the oncogenic p53DBD structural mutant G245S.

We used differential scanning fluorimetry to measure whether increased concentrations of CLR01 affected the thermodynamic stability of G245S-p53DBD. CLR01 concentrations below 100 μM did not affect the apparent T_m of G245S-p53DBD (Figure 3). At higher concentrations, CLR01 destabilized the protein. Therefore, we set 100 μM as the maximal concentration for further analysis. CLR03, which served as a negative control, had no effect on the apparent T_m of the protein, as expected.

CLR01 Induces Rapid Formation of Intermediate, β-Sheet-Rich, Mutant p53DBD Aggregates. Aggregation of p53DBD is accompanied by a conformational transition into amyloid-like structures characterized by a high β-sheet content that can be measured using ThT binding.[6] Alterations in the pH may influence aggregation rates dramatically.[6] Therefore, we measured the effect of increased concentrations of CLR01 or CLR03 on the pH of the solution and found that CLR01 or CLR03 caused little change in the pH up to the highest concentration examined, 100 μM (Figure S1 of the Supporting Information).

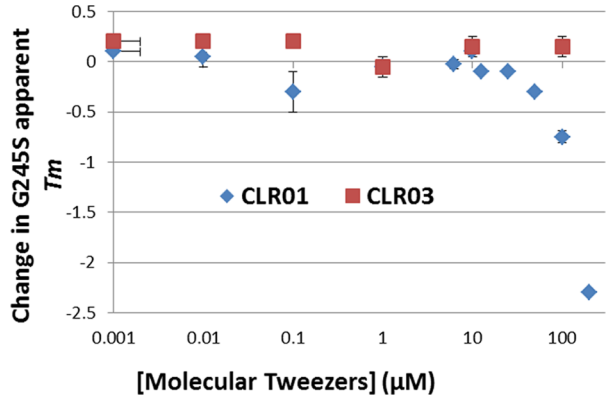

Figure 3. Effect of molecular tweezers on the thermostability of the p53DBD. The effect of the increased molar ratio of either CLR01 or CLR03 on stability of the G245S-p53DBD mutant was measured using differential scanning fluorimetry.

ThT binding is independent of the size of protein aggregates. Therefore, it is useful for monitoring the early stages of p53DBD aggregation.[5] Using this method, we found that at a protein:CLR molar ratio of 1:5, CLR01 rapidly enhanced ThT binding by G245S-p53DBD (Figure 4), suggesting induction of

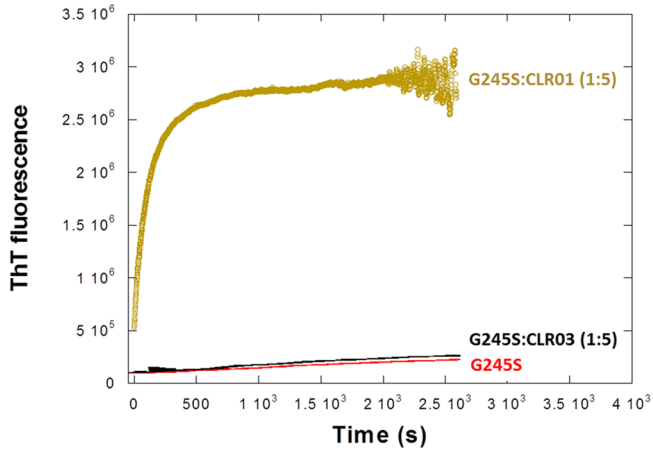

Figure 4. Effect of molecular tweezers on the early stage of p53DBD aggregation. The effect of CLR01 or CLR03 on the early stage of aggregation of G245S-p53DBD was monitored at 37 °C using ThT fluorescence (λ_{ex} = 450 nm; λ_{em} = 482 nm).

formation of a β-sheet-rich structure. This effect was similar to that reported previously by Sinha et al. for insulin, β_2-microglobulin, and TTR,[14] though the experiments in that study had a time resolution substantially lower than that measured here. Therefore, they observed a high-intensity ThT fluorescence signal already at the earliest time point measured, whereas we monitored the development of the signal during the first ~30 s.

Next, we used circular dichroism (CD) spectroscopy to evaluate the secondary structure of the G245S-p53DBD mutant in the presence of increased molar ratios of CLR01. In the absence of CLR01, G245S-p53DBD displayed typical α-helix-rich CD spectra characterized by minima at ~207 and 220 nm, in which the 207 nm minimum was slightly lower than that at 220 nm (Figure 5), as previously reported.[21] In the presence of CLR01, a shift was evident toward a β-sheet-rich structure, characterized by a single minimum at 216 nm (Figure 5). In

DOI: 10.1021/bi501092p
Biochemistry 2015, 54, 3729−3738

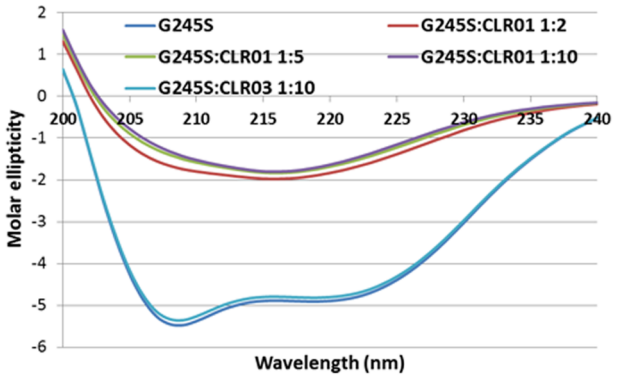

	Helix	Antiparallel	Parallel	Beta-Turn
G245S	63.5	2.7	3.1	12.9
G245S:CLR01 (1:2)	21.7	19.8	11.9	19.5
G245S:CLR01 (1:5)	18.4	23.8	12.8	17
G245S:CLR01 (1:10)	18.4	23.8	12.8	17
G245S:CLR03 (1:10)	42.4	6	6.6	15.6

Figure 5. Effect of molecular tweezers on the secondary structure of p53DBD. Far-UV CD spectra of G245S-p53DBD in the absence or presence of an increasing molar ratio of CLR01 or CLR03. CD spectra were recorded at 37 °C after incubation for 20 min. The table presents the percentage of secondary structure calculated using the CDNN software.[20]

contrast, CLR03 had no effect on the conformation of G245S-p53DBD, as expected. These CD results corroborated the ThT data.

We also used dot blots with antibody OC, which specifically recognizes β-sheet-rich amyloid fibrils,[22] to examine the effect of CLR01 on aggregation of G245S-p53DBD. We found that increased concentrations of CLR01 (up to 5-fold excess) resulted in a higher level of OC binding, suggesting enrichment of β-sheet-rich structures (Figure 6). To examine whether this

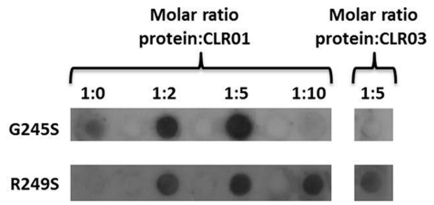

Figure 6. p53DBD aggregation monitored by dot blot with antibody OC. Dot blot was performed using the OC antibody with preformed aggregates of G245S-p53DBD or R249S-p53DBD in the absence or presence of an increasing molar ratio of CLR01 or CLR03.

effect was specific for the G245S mutant, we studied similarly an additional structural p53DBD mutant, R249S.[23] In the presence of CLR01, R249S-p53DBD also displayed enrichment of β-sheet-rich structures. This result indicated that the effect of CLR01 was not unique to G245S-p53DBD. Surprisingly, in the presence of CLR03, R249S-p53DBD, but not G245S-p53DBD, also showed a moderate increase in the level of OC binding, demonstrating a different behavior of the two p53DBD variants (Figure 6).

We examined further the effect of CLR01 on aggregation of G245S-p53DBD using static light scattering, which is most effective for monitoring intermediate-size assemblies. The experiments showed dose-dependent acceleration of the aggregation reaction, resulting both from shortening of the lag phase and from an increase in aggregate growth rate (Figure 7). At the highest molar ratio examined, 1:10 protein:CLR01,

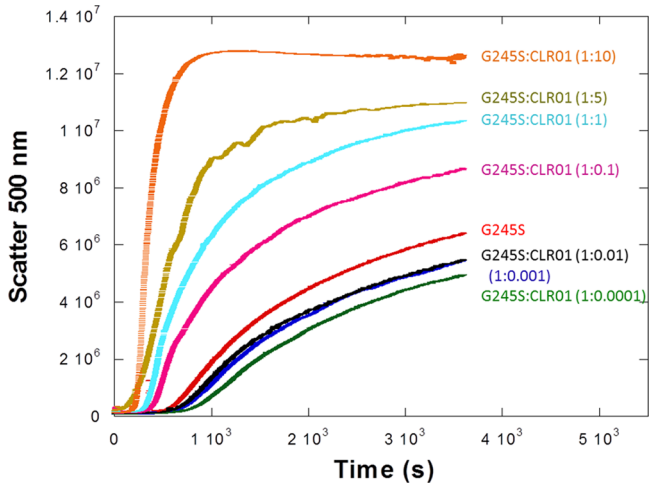

Figure 7. Effect of molecular tweezers on the intermediate stage of p53DBD aggregation. The effect of the increased molar ratio of CLR01 on the intermediate stage of aggregation of G245S-p53DBD was monitored at 37 °C, using static light scattering (λ = 500 nm).

the reaction plateaued at ~500 s. Together, the ThT fluorescence, CD spectral, OC binding, and static light scattering data suggest that when CLR01 binds to G245S-p53DBD, the protein rapidly forms β-sheet-rich, intermediate-size aggregates. In contrast, binding of CLR03 to G245S-p53DBD had no effect on the protein aggregation, as expected.

To further investigate the conformational changes of G245S-p53DBD or R249S-p53DBD induced by CLR01, we measured the change in fluorescence upon binding of ANS, a common probe for exposed hydrophobic regions in proteins.[24] When ANS is free in solution, its fluorescence emission is negligible, but once it binds to hydrophobic patches, its fluorescence emission increases.[25] Consequently, ANS has been used widely to characterize intermediate states of proteins such as the molten globule state.[26] We found that binding of CLR01 to p53DBD mutant G245S or R249S dramatically reduced ANS emission by ~6- or ~4-fold, respectively, compared to that of the untreated proteins. This low ANS emission was evident both by the rate and by the amplitude of ANS binding. This suggests that CLR01 reduces the level of exposure of hydrophobic residues in the protein already at the early stages of the folding−unfolding equilibrium of the p53DBD mutants, and further when aggregation is initiated. Interestingly, CLR03 had no effect on G245S-p53DBD, as expected, but slightly reduced the ANS emission of R249S-p53DBD (Figure 8), in agreement with the differences observed between the two p53DBD mutants in OC binding.

Collectively, our results suggest that CLR01 induces formation of β-sheet-rich structures in the p53DBD mutants studied and simultaneously inhibits the exposure of hydrophobic pockets in these proteins, presumably by inducing sequestration of hydrophobic patches through intermolecular association and formation of intermediate-size aggregates.

CLR01 Inhibits the Late Stages of Mutant p53DBD Aggregation. To monitor the effect of molecular tweezers on the rate of formation of the late stages of G245S-p53DBD or R249S-p53DBD aggregation and on the morphology of the resulting aggregates, proteins were incubated in the absence or

DOI: 10.1021/bi501092p
Biochemistry 2015, 54, 3729−3738

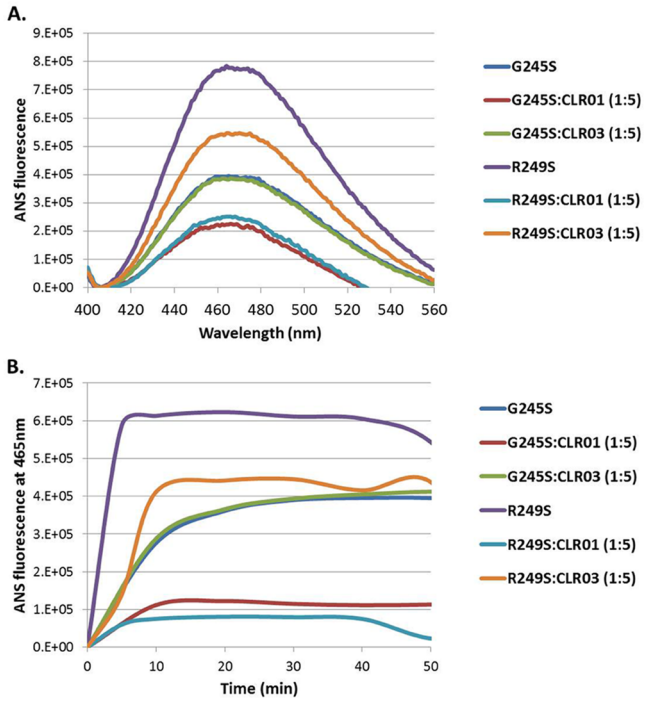

Figure 8. Effect of molecular tweezers on the early stage of p53DBD folding/unfolding kinetics using ANS. The effect of a 5-fold excess of CLR01 or CLR03 on the early stage of conformational change kinetics of G245S-p53DBD or R249S-p53DBD was monitored at 37 °C using ANS fluorescence (λ_{ex} = 350 nm; λ_{em} = 400−560 nm). (A) ANS fluorescence spectra after incubation for 20 min at 37 °C. (B) λ_{max} (465 nm) plotted as a function of temperature.

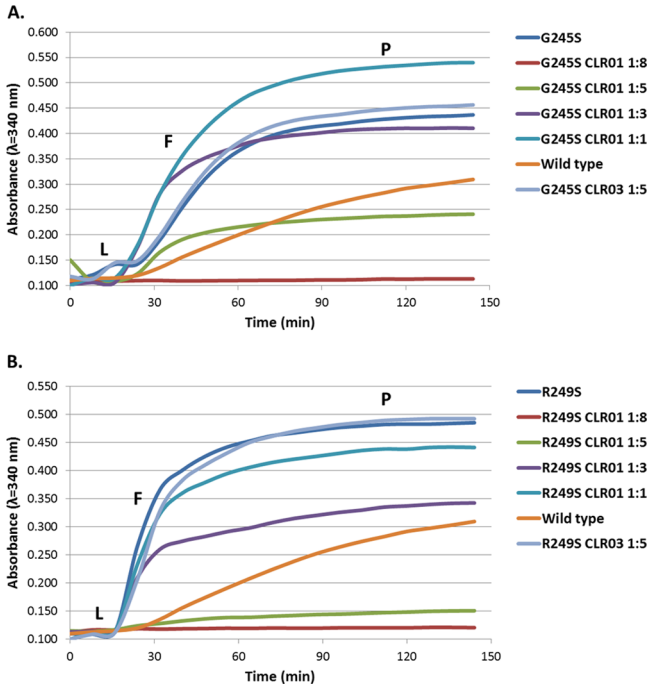

Figure 9. Effect of molecular tweezers on the late stage of p53DBD aggregation. The effect of the increased molar ratio of CLR01 on the late stage of aggregation of (A) G245S-p53DBD and (B) R247S-p53DBD was monitored at 37 °C, using turbidity (λ = 340 nm). L indicates the lag phase, F the fast growth of aggregates, and P the final stage of the aggregation reaction.

presence of increasing concentrations of MTs and the reaction was monitored using turbidity and transmission electron microscopy (TEM). R249S-p53DBD exhibited a degree of aggregation faster and higher than that of G245S-p53DBD, correlating with the kinetics observed in the ANS binding assay (Figure 8 and ref 3).

Consistent with the results obtained in the ThT, CD, OC antibody binding, and static light scattering experiments described above, the initial turbidity of the solution in the presence of a 1:1 molar ratio of CLR01 was higher than the turbidity of G245S-p53DBD or the same as that of R249S-p53DBD alone. However, whereas in the solution containing G245S-p53DBD on its own, a lag phase of ∼25 min was observed before the turbidity increased, in the presence of CLR01 the turbidity decreased in the first 15 min and then began to increase (Figure 9A). Interestingly, at a 1:1 protein:CLR01 molar ratio, the amplitude of the turbidity was higher than that of G245S-p53DBD alone, whereas at a 1:2 protein:CLR01 molar ratio, the turbidity amplitude was similar to that of G245S-p53DBD alone.

Increasing the concentration of CLR01 to a 1:5 protein:CLR01 molar ratio resulted in a decreased turbidity, and at a 1:8 protein:CLR01 molar ratio, no change in turbidity was observed throughout the experiment, suggesting that at this concentration, aggregation was inhibited completely (Figure 9). Similar results were observed with R249S-p53DBD, which is less folded than G245S.[9] CLR01 inhibited the aggregation of R249S-p53DBD in a dose-dependent manner starting at a 1:1 ratio (Figure 9), though in this case, CLR01 inhibited the growth rate of R249S-p53DBD, but not its nucleation rate. CLR03 did not affect the aggregation of the p53DBD mutants measured by turbidity, as expected (Figure 9). These results recapitulate the previously reported inhibitory effect of CLR01 on the aggregation of other amyloidogenic proteins.[14,27]

TEM analysis indicated that in the presence of CLR01 the p53DBD mutant aggregates were smaller and more dispersed (Figure 10). Higher-magnification images revealed occasional small, curvilinear fibrils (Figure 10C). Interestingly, at a 1:10 protein:CLR01 molar ratio, the aggregates were less dispersed. CLR03 had no effect on G245S-p53DBD aggregates but did reduce the number of R249S-p53DBD aggregates. Both MTs had little effect on the morphology of the aggregates (Figure 10).

Taken together, the results described above indicate that CLR01 enhances self-assembly of the p53DBD mutants examined into β-sheet-rich structures. Apparently, however, these structures are "off pathway" for formation of typical later-stage p53DBD mutant aggregates because the kinetics of formation of the later-stage aggregates and the final amount of these aggregates are reduced in the presence of CLR01 in a dose-dependent manner. The modulatory activity of CLR01 requires the hydrophobic side arms of the molecular tweezer, because the negative control CLR03 shows little or no effect on the aggregation of the p53DBD mutants.

CLR01 Reduces the Toxicity of p53DBD Aggregates. The next important question was whether the assemblies stabilized by CLR01 were cytotoxic. Introduction of *in vitro* preformed aggregates of p53DBD mutants into cells has been reported to reduce cell viability,[6] like other amyloidogenic proteins.[14,28] We examined next whether the MTs affect this cytotoxicity in H1299 lung carcinoma cells. CLR01 was reported to be nontoxic in differentiated PC-12 cells up to 200 μM and to induce mild toxicity at 400 μM.[14] However,

DOI: 10.1021/bi501092p
Biochemistry 2015, 54, 3729−3738

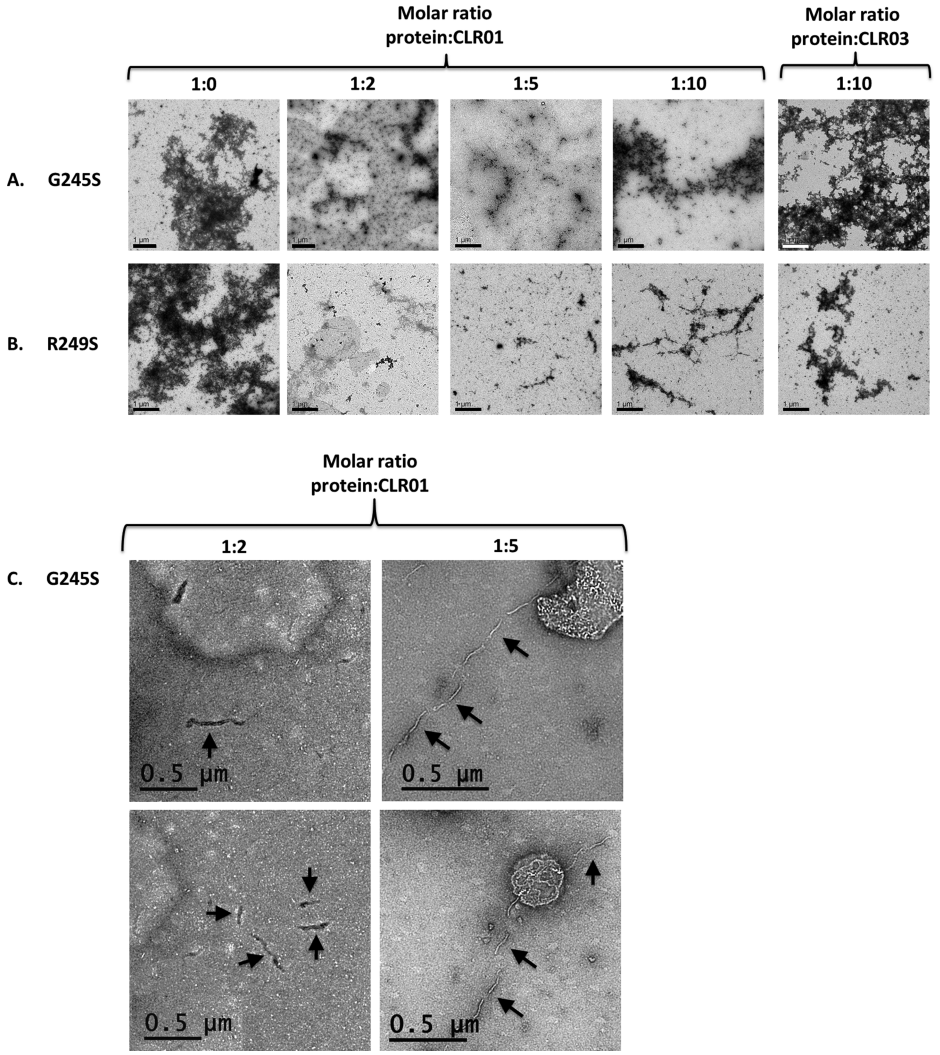

Figure 10. Effect of molecular tweezers on p53DBD morphology. Transmission electron micrographs of the aggregates of (A) G245S-p53DBD or (B) R249S-p53DBD at 37 °C in the absence or presence of an increasing molar ratio of CLR01 or a 1:10 molar ratio of CLR03, respectively. The scale bar is 1 μm. (C) Magnified view of areas with apparent fibrils of G245S-p53DBD and CLR01 in a 1:2 or 1:5 molar ratio. The scale bar is 0.5 μm.

toxicity can vary depending on the cell line used. Therefore, we tested the effect of CLR01 and CLR03 on H1299 cells. We found that in agreement with the results reported in PC-12 cells and primary neurons,[29] CLR01 at 10−100 μM and CLR03 at 100 μM were not cytotoxic (Figure S2 of the Supporting Information).

To test the effect of the MTs on cytotoxicity induced by mutant p53DBD, we incubated preformed G245S-p53DBD or R249S-p53DBD aggregates with CLR01 at molar ratios from 1:2 to 1:10 or CLR03 at 1:10 and applied the mixtures to H1299 cells. CLR01 protected the cells significantly from the harmful effect of G245S-p53DBD or R249S-p53DBD aggregates (Figure 11). The protective effect displayed hormetic behavior as at a 1:10 molar ratio, lower, nonsignificant protection was observed. Thus, the maximal protection was observed at 1:5 and 1:2 molar ratios for G245S-p53DBD and R249S-p53DBD, respectively. This was not caused by toxicity of CLR01 itself, as shown in Figure S2 of the Supporting Information, and at this point, the basis for this behavior is not clear. Interestingly, CLR03 had a significant, dose-independent rescue effect on the viability of R249S-p53DBD-treated cells. This may reflect its moderate effect on R249S-p53DBD observed in the OC, ANS binding, and TEM.

DISCUSSION

Aggregation of p53 conformational mutants has gained recent interest because it accounts for both their dominant-negative and gain-of-toxic-function effects. Our findings that aggregation of p53 mutants converts their native conformation into a β-sheet-rich, amyloid-like structure are in line with recent data reported by other groups that used Congo red staining and ThT fluorescence for monitoring β-sheet structures, as well as recognition by antibody A11, which binds specifically to oligomers of amyloidogenic proteins.[5,6] Thus, cancers resulting from misfolded p53 may belong to the broad spectrum of diseases called amyloidoses, including Alzheimer's disease, Parkinson's disease, prion diseases, and amyotrophic lateral sclerosis, which are caused by abnormal misfolding and aggregation of amyloidogenic proteins.[30−32] This novel view of p53 aggregation suggests that therapeutics based on modulating aggregation of amyloidogenic proteins also may

DOI: 10.1021/bi501092p
Biochemistry 2015, 54, 3729−3738

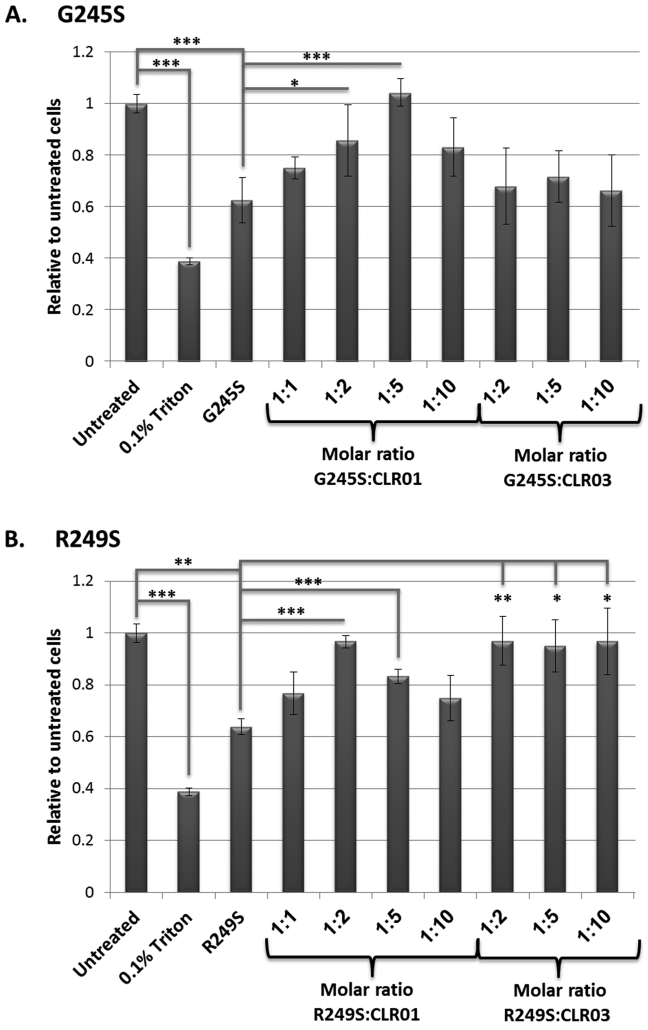

Figure 11. Effect of molecular tweezers on p53DBD-induced cytotoxicity. H1299 cells were grown for 24 h. Cells were incubated for 24 h with preformed aggregates of G245S-p53DBD or R249S-p53DBD in the absence or presence of an increasing molar ratio of CLR01 or CLR03. Cell viability was measured using the XTT assay. Triton (0.1%) was used as a positive control. (A) G245S-p53DBD. (B) R249S-p53DBD. Data are expressed as the percent change compared to the relevant control. p values were calculated by using the t test: $^{*}p < 0.1$, $^{**}p < 0.05$, and $^{***}p < 0.001$.

be effective against p53 aggregation and the cytotoxicity of the resulting aggregates.

The proposed mechanism of action of CLR01 is binding selectively to exposed Lys residues (and to a lesser extent to Arg residues), thereby disrupting hydrophobic and electrostatic interactions that mediate oligomerization and aggregation of amyloidogenic proteins and preventing their toxicity.[33] The selectivity of the compound is based on the fact that the forces controlling the abnormal aggregation process are relatively weak; hence, the oligomers are unstable and are in a dynamic quasi-equilibrium. The binding of CLR01 is highly labile[34] and of moderate (micromolar) affinity and therefore does not interfere with the structure or function of normal proteins, whose three-dimensional structure has been optimized by millions of years of evolution.

The recent suggestion that p53 aggregates into amyloid-like structures[5,12,30−32,35] prompted us to examine if CLR01 could inhibit the aggregation and toxicity of "conformational" p53 mutants. In the 393-residue sequence of the native p53 monomer, there are 20 Lys (5.1%) and 26 Arg (6.6%) residues, whereas in the 179-residue DBD, the Arg content is higher, 8.9%, and the Lys content is 2.2%. These numbers are on par with those of amyloidogenic proteins studied previously[14] and suggested that CLR01 might be able to inhibit the aggregation of mutant p53 and the toxicity of the aggregates.

Of the amyloidogenic proteins for which CLR01's inhibitory activity was studied previously,[14,27,36,37] Aβ40, Aβ42, tau, α-synuclein, and islet amyloid polypeptide are intrinsically disordered, insulin, β_2-microglobulin, and TTR are natively structured, and calcitonin is a relatively short peptide that is partially structured in aqueous solution. Analysis of the behavior of the mixture of each of these proteins with CLR01 in ThT fluorescence or turbidity experiments[14] revealed a pattern. For intrinsically disordered proteins, initial ThT binding was minimal and the fluorescence at the beginning of the aggregation reaction was close to background values. In contrast, for the natively structured proteins, the initial ThT fluorescence/turbidity signal was substantially higher in the presence of CLR01 than in its absence, suggesting that binding of CLR01 rapidly induced formation of aggregates in which the β-sheet content was increased relative to that of the CLR01-unbound state. In the case of calcitonin, the increase in the initial ThT fluorescence was small relative to the structured proteins, as would be expected for a partially structured peptide.[14]

Because like insulin, β_2-microglobulin, and TTR, p53 has a well-defined stable structure, we expected that upon interaction with G245S-p53DBD or R249S-p53DBD, CLR01 would induce formation of β-sheet-rich aggregates. This was indeed what we found. Turbidity measurements showed that at the initial time points, larger aggregates were present in samples of G245S-p53DBD or R249S-p53DBD in the presence of CLR01 than in its absence (Figure 9). Therefore, we conducted ThT fluorescence, CD spectra, OC binding, ANS fluorescence, and static light scattering experiments with a time resolution higher than that of the experiments conducted previously with other proteins or the turbidity measurements performed here. Using the higher time resolution, we observed the rapid formation of β-sheet-rich, intermediate-size, G245S-p53DBD−CLR01 complexes within ∼1 min of mixing the protein and the molecular tweezer (Figures 4 and 7). Examination by TEM, and static light scattering experiments, showed that the size and morphology of the initial G245S-p53DBD and R249S-p53DBD aggregates formed in the absence or presence of CLR01 were similar (Figure 10), suggesting that the differences between the two types of aggregates were subtle and deciphering these differences would require higher spatial-resolution methods.

Like that of other amyloidogenic proteins, p53 aggregation is thought to occur via nucleation-dependent polymerization,[5] characterized by a slow nucleation step followed by fast growth of aggregates.[38] Our observations support this model. We found that the initial stage of aggregation of the mutant p53 examined occurs at a slow rate followed by a rapid phase of aggregation evidenced by a steep slope (indicated as L and F, respectively, in Figure 9). The final stage is a decrease in the rate of aggregation and ultimately a plateau, as the system reaches equilibrium (P in Figure 9). During the final slow step, formation of larger aggregates by association of smaller ones is thought to be a secondary mechanism, though it is difficult to distinguish kinetically from the growth of individual aggregates

DOI: 10.1021/bi501092p
Biochemistry 2015, 54, 3729−3738

by currently available techniques. Our data suggest that binding of CLR01 greatly accelerated a nucleation-like phase of G245S-p53DBD or R249S-p53DBD, but the protein−CLR01 assemblies and/or nuclei had an off-pathway structure distinct from that of these proteins alone. The heteroassemblies of G245S-p53DBD or R249S-p53DBD with CLR01 did not promote further growth or propagation of the β-sheet structure. Importantly, these heteroassemblies had reduced toxicity relative to that of those formed by G245S-p53DBD or R249S-p53DBD alone.

Cellular effects of p53 aggregation in cancer are associated with cell survival and proliferation rather than with cell death, in contrast to neurodegeneration. However, our cell viability results support recent findings showing that *in vitro* preformed aggregates of mutant p53 are cytotoxic[13] and suggest that CLR01 can protect cells from this cytotoxicity, in agreement with its effect on other amyloidogenic proteins.

Interestingly, though CLR03 was used as a negative control and was not expected to affect the aggregation or toxicity of the p53DBD mutants, we found that it moderately increased OC binding and decreased ANS binding, selectively to R249S-p53DBD. In correlation with these data, CLR03 also showed moderate, dose-independent protection of H1299 cells against the toxicity of R249S-p53DBD, suggesting that it might promote formation of nontoxic aggregates by a currently unknown mechanism. In most of the studies reported to date, CLR03 was found to behave as a negative control, i.e., did not affect the proteins under study where CLR01 had a clear impact. This was the case also in all the experiments we performed using G245S-p53DBD. In a recent study, CLR03 was found to induce moderate enhancement of oligomerization of Aβ40 and Aβ42 using ion-mobility spectroscopy−mass spectrometry,[35] similar to its effect on G245S-p53DBD. The basis for this activity currently is unknown.

Conformational p53 mutants co-aggregate with wild-type p53 in cells.[12] If this were also the case *in vivo*, this aggregation would result in even lower availability of the wild-type protein, and a higher propensity for malignant cell proliferation. Ideally, inhibition of the abnormal aggregation of mutant p53 would lead to degradation of the misfolded, mutant protein, and release of the normal, wild-type protein, increasing its availability for DNA transcription regulation. Our data suggest that the use of aggregation modulators, such as CLR01, could lead to selective degradation of misfolded p53, thereby increasing the availability of normal p53. Determining the extent of the protective effect provided by inhibiting the aggregation of mutant p53 will require further investigation.

■ ASSOCIATED CONTENT

Supporting Information

Supplementary figures showing the effect of increased concentrations of molecular tweezers on the pH of the buffer (Figure S1) and on cell viability (Figure S2). The Supporting Information is available free of charge on the ACS Publications website at DOI: 10.1021/bi501092p.

■ AUTHOR INFORMATION

Corresponding Author

*Department of Molecular Microbiology and Biotechnology, Tel Aviv University, Tel Aviv 69978, Israel. Phone: ++972-3-6409835. Fax: ++972-3-640-9407. E-mail: dsegal@post.tau.ac.il.

Author Contributions

G.H. and M.D.S. contributed equally to this work.

Funding

This research was supported in part by grants from the Israel Science Foundation and the U.S. Department of Defense (CDMRP) to D.S. and by the UCLA Jim Easton Consortium for Drug Discovery and Biomarker development to G.B. G.H. acknowledges travel fellowships from Tel-Aviv University Center for Nanoscience and Nanotechnology.

Notes

The authors declare no competing financial interest.

■ ACKNOWLEDGMENTS

We are indebted to Prof. Alan R. Fersht and Dr. Andreas C. Joerger (University of Cambridge, Cambridge, U.K.) for generously hosting G.H. during part of this project and for their invaluable advice.

■ REFERENCES

(1) Lane, D. P. (1992) Cancer. p53, guardian of the genome. *Nature 358*, 15−16.

(2) Bullock, A. N., Henckel, J., DeDecker, B. S., Johnson, C. M., Nikolova, P. V., Proctor, M. R., Lane, D. P., and Fersht, A. R. (1997) Thermodynamic stability of wild-type and mutant p53 core domain. *Proc. Natl. Acad. Sci. U.S.A. 94*, 14338−14342.

(3) Friedler, A., Veprintsev, D. B., Hansson, L. O., and Fersht, A. R. (2003) Kinetic instability of p53 core domain mutants: Implications for rescue by small molecules. *J. Biol. Chem. 278*, 24108−24112.

(4) Bullock, A. N., Henckel, J., and Fersht, A. R. (2000) Quantitative analysis of residual folding and DNA binding in mutant p53 core domain: Definition of mutant states for rescue in cancer therapy. *Oncogene 19*, 1245−1256.

(5) Wilcken, R., Wang, G., Boeckler, F. M., and Fersht, A. R. (2012) Kinetic mechanism of p53 oncogenic mutant aggregation and its inhibition. *Proc. Natl. Acad. Sci. U.S.A. 109*, 13584−13589.

(6) Ano Bom, A. P., Rangel, L. P., Costa, D. C., de Oliveira, G. A., Sanches, D., Braga, C. A., Gava, L. M., Ramos, C. H., Cepeda, A. O., Stumbo, A. C., De Moura Gallo, C. V., Cordeiro, Y., and Silva, J. L. (2012) Mutant p53 aggregates into prion-like amyloid oligomers and fibrils: Implications for cancer. *J. Biol. Chem. 287*, 28152−28162.

(7) Ishimaru, D., Andrade, L. R., Teixeira, L. S., Quesado, P. A., Maiolino, L. M., Lopez, P. M., Cordeiro, Y., Costa, L. T., Heckl, W. M., Weissmuller, G., Foguel, D., and Silva, J. L. (2003) Fibrillar aggregates of the tumor suppressor p53 core domain. *Biochemistry 42*, 9022−9027.

(8) Olivier, M., Eeles, R., Hollstein, M., Khan, M. A., Harris, C. C., and Hainaut, P. (2002) The IARC TP53 database: New online mutation analysis and recommendations to users. *Hum. Mutat. 19*, 607−614.

(9) Joerger, A. C., and Fersht, A. R. (2007) Structure-function-rescue: The diverse nature of common p53 cancer mutants. *Oncogene 26*, 2226−2242.

(10) Joerger, A. C., and Fersht, A. R. (2008) Structural biology of the tumor suppressor p53. *Annu. Rev. Biochem. 77*, 557−582.

(11) Joerger, A. C., Ang, H. C., and Fersht, A. R. (2006) Structural basis for understanding oncogenic p53 mutations and designing rescue drugs. *Proc. Natl. Acad. Sci. U.S.A. 103*, 15056−15061.

(12) Xu, J., Reumers, J., Couceiro, J. R., De Smet, F., Gallardo, R., Rudyak, S., Cornelis, A., Rozenski, J., Zwolinska, A., Marine, J. C., Lambrechts, D., Suh, Y. A., Rousseau, F., and Schymkowitz, J. (2011) Gain of function of mutant p53 by coaggregation with multiple tumor suppressors. *Nat. Chem. Biol. 7*, 285−295.

(13) Forget, K. J., Tremblay, G., and Roucou, X. (2013) p53 aggregates penetrate cells and induce the co-aggregation of intracellular p53. *PLoS One 8*, e69242.

(14) Sinha, S., Lopes, D. H., Du, Z., Pang, E. S., Shanmugam, A., Lomakin, A., Talbiersky, P., Tennstaedt, A., McDaniel, K., Bakshi, R.,

DOI: 10.1021/bi501092p
Biochemistry 2015, 54, 3729−3738

Kuo, P. Y., Ehrmann, M., Benedek, G. B., Loo, J. A., Klärner, F. G., Schrader, T., Wang, C., and Bitan, G. (2011) Lysine-specific molecular tweezers are broad-spectrum inhibitors of assembly and toxicity of amyloid proteins. *J. Am. Chem. Soc. 133*, 16958−16969.
(15) Attar, A., Chan, W. T., Klarner, F. G., Schrader, T., and Bitan, G. (2014) Safety and pharmacological characterization of the molecular tweezer CLR01: A broad-spectrum inhibitor of amyloid proteins' toxicity. *BMC Pharmacol. Toxicol. 15*, 23.
(16) Talbiersky, P., Bastkowski, F., Klärner, F. G., and Schrader, T. (2008) Molecular clip and tweezer introduce new mechanisms of enzyme inhibition. *J. Am. Chem. Soc. 130*, 9824−9828.
(17) Prabhudesai, S., Sinha, S., Attar, A., Kotagiri, A., Fitzmaurice, A. G., Lakshmanan, R., Ivanova, M. I., Loo, J. A., Klarner, F. G., Schrader, T., Stahl, M., Bitan, G., and Bronstein, J. M. (2012) A novel "molecular tweezer" inhibitor of α-synuclein neurotoxicity in vitro and in vivo. *Neurotherapeutics 9*, 464−476.
(18) Attar, A., Ripoli, C., Riccardi, E., Maiti, P., Li Puma, D. D., Liu, T., Hayes, J., Jones, M. R., Lichti-Kaiser, K., Yang, F., Gale, G. D., Tseng, C. H., Tan, M., Xie, C. W., Straudinger, J. L., Klärner, F. G., Schrader, T., Frautschy, S. A., Grassi, C., and Bitan, G. (2012) Protection of primary neurons and mouse brain from Alzheimer's pathology by molecular tweezers. *Brain 135*, 3735−3748.
(19) Ferreira, N., Pereira-Henriques, A., Attar, A., Klärner, F. G., Schrader, T., Bitan, G., Gales, L., Saraiva, M. J., and Almeida, M. R. (2014) Molecular tweezers targeting transthyretin amyloidosis. *Neurotherapeutics 11*, 450−461.
(20) Bohm, G., Muhr, R., and Jaenicke, R. (1992) Quantitative analysis of protein far UV circular dichroism spectra by neural networks. *Protein Eng. 5*, 191−195.
(21) Merabet, A., Houlleberghs, H., Maclagan, K., Akanho, E., Bui, T. T., Pagano, B., Drake, A. F., Fraternali, F., and Nikolova, P. V. (2010) Mutants of the tumour suppressor p53 L1 loop as second-site suppressors for restoring DNA binding to oncogenic p53 mutations: Structural and biochemical insights. *Biochem. J. 427*, 225−236.
(22) Kayed, R., Head, E., Sarsoza, F., Saing, T., Cotman, C. W., Necula, M., Margol, L., Wu, J., Breydo, L., Thompson, J. L., Rasool, S., Gurlo, T., Butler, P., and Glabe, C. G. (2007) Fibril specific, conformation dependent antibodies recognize a generic epitope common to amyloid fibrils and fibrillar oligomers that is absent in prefibrillar oligomers. *Mol. Neurodegener. 2*, 18.
(23) Joerger, A. C., and Fersht, A. R. (2007) Structural biology of the tumor suppressor p53 and cancer-associated mutants. *Adv. Cancer Res. 97*, 1−23.
(24) Seifert, T., Bartholmes, P., and Jaenicke, R. (1984) Binding of the fluorescent dye 8-anilinonaphthalene 1-sulfonic acid to the native and pressure dissociated β 2-dimer of tryptophan synthase from *Escherichia coli*. *Z. Naturforsch. 39C*, 1008−1011.
(25) Semisotnov, G. V., Rodionova, N. A., Razgulyaev, O. I., Uversky, V. N., Gripas, A. F., and Gilmanshin, R. I. (1991) Study of the "molten globule" intermediate state in protein folding by a hydrophobic fluorescent probe. *Biopolymers 31*, 119−128.
(26) Shmueli, M. D., Schnaider, L., Rosenblum, D., Herzog, G., Gazit, E., and Segal, D. (2013) Structural Insights into the Folding Defects of Oncogenic pVHL Lead to Correction of Its Function In Vitro. *PLoS One 8*, e66333.
(27) Prabhudesai, S., Sinha, S., Attar, A., Kotagiri, A., Fitzmaurice, A. G., Lakshmanan, R., Ivanova, M. I., Loo, J. A., Klärner, F. G., Schrader, T., Stahl, M., Bitan, G., and Bronstein, J. M. (2012) A novel "molecular tweezer" inhibitor of α-synuclein neurotoxicity in vitro and in vivo. *Neurotherapeutics 9*, 464−476.
(28) Rahimi, F., and Bitan, G. (2012) The structure and function of fibrillar and oligomeric assemblies of amyloidogenic proteins. In *Non-fibrillar Amyloidogenic Protein Assemblies−Common Cytotoxins Underlying Degenerative Diseases*; Rahimi, F., and Bitan, G., Eds.; Springer Science+Media B.V., Dordrecht, pp 1−36.
(29) Sinha, S., Du, Z., Maiti, P., Klärner, F. G., Schrader, T., Wang, C., and Bitan, G. (2012) Comparison of three amyloid assembly inhibitors: The sugar *scyllo*-inositol, the polyphenol epigallocatechin gallate, and the molecular tweezer CLR01. *ACS Chem. Neurosci. 3*, 451−458.
(30) Silva, J. L., Gallo, C. V., Costa, D. C., and Rangel, L. P. (2014) Prion-like aggregation of mutant p53 in cancer. *Trends Biochem. Sci.*, in press.
(31) Silva, J. L., Rangel, L. P., Costa, D. C., Cordeiro, Y., and De Moura Gallo, C. V. (2013) Expanding the prion concept to cancer biology: Dominant-negative effect of aggregates of mutant p53 tumour suppressor. *Biosci. Rep. 33*, e00054.
(32) Rangel, L. P., Costa, D. C., Vieira, T. C., and Silva, J. L. (2014) The aggregation of mutant p53 produces prion-like properties in cancer. *Prion 8*, 75−84.
(33) Attar, A., and Bitan, G. (2014) Disrupting self-assembly and toxicity of amyloidogenic protein oligomers by "molecular tweezers": From the test tube to animal models. *Curr. Pharm. Des. 20*, 2469−2483.
(34) Bier, D., Rose, R., Bravo-Rodriguez, K., Bartel, M., Ramirez-Anguita, J. M., Dutt, S., Wilch, C., Klärner, F. G., Sanchez-Garcia, E., Schrader, T., and Ottmann, C. (2013) Molecular tweezers modulate 14-3-3 protein-protein interactions. *Nat. Chem. 5*, 234−239.
(35) Wang, G., and Fersht, A. R. (2012) First-order rate-determining aggregation mechanism of p53 and its implications. *Proc. Natl. Acad. Sci. U.S.A. 109*, 13590−13595.
(36) Zheng, X., Liu, D., Klarner, F. G., Schrader, T., Bitan, G., and Bowers, M. T. (2015) Amyloid β-Protein Assembly: The Effect of Molecular Tweezers CLR01 and CLR03. *J. Phys. Chem. B 119*, 4831−4841.
(37) Lopes, D. H., Attar, A., Nair, G., Hayden, E., Du, Z., McDaniel, K., Dutt, S., Bravo-Rodriguez, K., Mittal, S., Klarner, F. G., Wang, C., Sanchez-Garcia, E., Schrader, T., and Bitan, G. (2015) Molecular tweezers inhibit islet amyloid polypeptide assembly and toxicity by a new mechanism. *ACS Chem. Biol.*, DOI: 10.1021/acschembio.5b00146.
(38) Jarrett, J. T., and Lansbury, P. T., Jr. (1993) Seeding "one-dimensional crystallization" of amyloid: A pathogenic mechanism in Alzheimer's disease and scrapie? *Cell 73*, 1055−1058.

DOI: 10.1021/bi501092p
Biochemistry 2015, 54, 3729−3738